J. Biomater. Sci. Polymer Edn, Vol. 19, No. 9, pp. 1143–1157 (2008)

Also available online - www.brill.nl/jbs

Furan-functionalized co-polymers for targeted drug delivery: characterization, self-assembly and drug encapsulation

MENG SHI [1,2,3] and MOLLY S. SHOICHET [1,2,3,4,*]

[1] *Department of Chemical Engineering and Applied Chemistry, University of Toronto, Toronto, Ontario, Canada M5S 3E1*
[2] *Institute for Biomaterials and Biomedical Engineering, University of Toronto, Toronto, Ontario, Canada M5S 3E1*
[3] *Terrence Donnelly Centre for Cellular and Biomolecular Research, 160 College Street, Toronto, Ontario, Canada M5S 3E1*
[4] *Department of Chemistry, University of Toronto, Toronto, Ontario, Canada M5S 3E1*

Received 10 August 2007; accepted 9 December 2007

Abstract—We have previously reported furan-maleimide Diels–Alder chemistry as a new methodology to couple maleimide-modified antibodies on furan-functionalized polymeric carriers in the preparation of immuno-nanoparticles for targeted drug delivery. In this report, we focus on the characterization, self-assembly behavior and drug encapsulation of two types of furan-functionalized co-polymers: poly(2-methyl, 2-carboxytrimethylene carbonate-*co*-D,L-lactide)-furan (poly(TMCC-*co*-LA)-furan) and poly(2-methyl, 2-carboxytrimethylene carbonate-*co*-D,L-lactide)-*graft*-poly(ethylene glycol)-furan (poly(TMCC-*co*-LA)-*g*-PEG-furan). The co-polymers were synthesized by modifying the carboxylic acid groups on the poly(TMCC-*co*-LA) backbone by either furfurylamine or PEG-furan to generate either linear co-polymers of poly(TMCC-*co*-LA)-furan with furan pendant groups or graft co-polymers of poly(TMCC-*co*-LA)-*g*-PEG-furan with furan-terminated PEG grafts, respectively. Using a membrane dialysis method, both of the co-polymers were self-assembled into nanoparticles in aqueous environments driven by the hydrophobic association among polymer chains. The hydrophobic domains in the nanoparticles were confirmed by the incorporation of pyrene molecules and the critical aggregation concentrations were determined to be approximately 5×10^{-5} mM for poly(TMCC-*co*-LA)-furan and 2×10^{-4} mM for poly(TMCC-*co*-LA)-*g*-PEG-furan. By the addition of borate buffer in the organic solvent used to dissolve the co-polymers in the dialysis procedure, we were able to control the size of the nanoparticles: 54–169 nm for poly(TMCC-*co*-LA)-furan and 28–283 nm for poly(TMCC-*co*-LA)-*g*-PEG-furan. This unique feature can be explained by the ionization of carboxylic acid groups along the co-polymer backbone. A hydrophobic anticancer drug, doxorubicin (DOX), was encapsulated within the nanoparticles, with the larger size nanoparticles in-

*To whom correspondence should be addressed at the Terence Donnelly Centre for Cellular and Biomolecular Research. Tel.: (1-416) 978-1460; Fax: (1-416) 978-4317; e-mail: molly@ecf.utoronto.ca

corporating greater amounts of DOX. Combining the strategy of antibody-mediated targeting, these self-assembled nanoparticles have potential as efficient anti-cancer drug carriers.

Key words: Amphiphilic co-polymer; drug delivery; polymeric nanoparticles; self-assembly.

INTRODUCTION

Self-assembling systems from polymeric amphiphiles, such as amphiphilic di-block or tri-block co-polymers, hydrophobically modified water-soluble polymers and graft co-polymers, have been developed for biomedical applications [1–10]. The formation of micellar structures by self-assembly of amphiphilic polymers in aqueous media has been well established [1, 3, 10, 11]. Upon contact with aqueous environments, these amphiphilic polymers spontaneously form micellar aggregates through inter- or intramolecular association during which drug molecules are encapsulated. Self-assembled polymeric nanoparticles have many advantages as highly efficient drug-delivery vehicles including nanoscale size, controlled composition and capacity to encapsulate a wide range of drug molecules [1, 3, 8, 12, 13]. In particular, polymeric nanoparticles provide a wide opportunity for functionalization and versatility by tuning materials properties through polymer synthesis [2, 4, 7, 8, 14–18]. For example, functional components in hydrophobic segments incorporate pH/temperature-responsive strategies into drug-delivery systems whose structure and property alter in response to external stimuli [14, 17]. Functional groups located at the termini of hydrophilic segments enable the conjugation of targeting molecules for the purpose of targeted drug delivery [2, 4, 7, 8, 18]. Polymeric amphiphiles continue to be developed for drug delivery due to their unique structure–property relationship.

Active targeting of drugs to specific regions of the body, for example cancer cells that overexpress specific receptors, has become one of the most important objectives for the next generation of drug-delivery systems [4, 7, 8, 18, 19]. By covalently coupling various targeting ligands, these smart drug-delivery systems are capable of targeting specific cell types exclusively through ligand–receptor interactions. Recently, we have reported a new conjugation methodology of Diels–Alder (DA) chemistry to couple antibodies to polymeric nanoparticles for the preparation of antibody-mediated drug-delivery vehicles [7]. The reaction between furan-functionalized nanoparticles and maleimide-modified antibodies has been demonstrated to occur under mild conditions with high coupling efficiency and preserved antibody bioactivity [7]. The methodology has opened a new window for furan-functionalized polymers to create antibody-conjugated delivery vehicles for targeted drug delivery.

In this study, we report the synthesis, characterization and self-assembly of two types of furan-functionalized co-polymers, one without and one with poly(ethylene glycol) (PEG), poly(2-methyl, 2-carboxy trimethylene carbonate-*co*-D,L-lactide)-furan (poly(TMCC-*co*-LA)-furan) and poly(2-methyl, 2-carboxy trimethylene car-

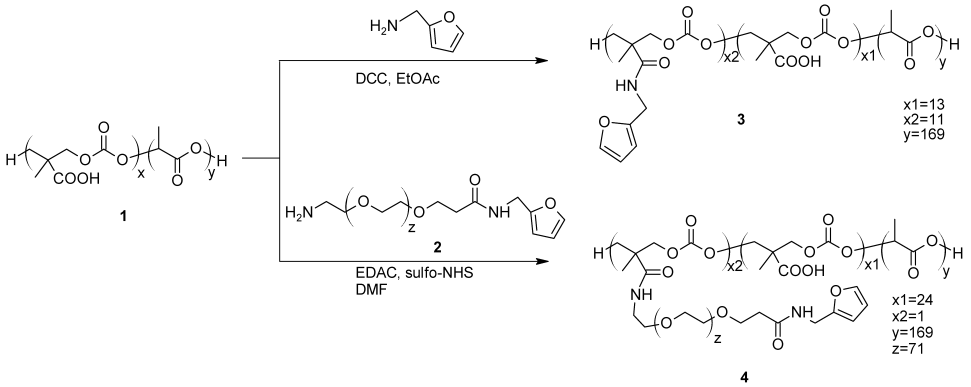

Scheme 1. Synthesis of furan-functionalized co-polymers poly(TMCC-*co*-LA)-furan (3) and poly(TMCC-*co*-LA)-*g*-PEG-furan (4).

bonate-*co*-D,L-lactide)-*graft*-poly(ethylene glycol)-furan ((poly(TMCC-*co*-LA)-*g*-PEG-furan) (see Scheme 1 for synthesis and chemical structure). We describe how the self-assembly process can be controlled to yield nanoparticles of different diameters and how this in turn affects doxorubicin (DOX) encapsulation.

MATERIALS AND METHODS

Materials

N-Hydroxysulfosuccinimide (Sulfo-NHS) was obtained from Pierce Biotechnology (Rockford, IL, USA). *tert*-Butoxycarbonyl protected amine-PEG-activated acid (BocNH-PEG-NHS) was purchased from Nektar Therapeutics (Birmingham, AL, USA). Dialysis membranes were purchased from Spectrum® Laboratories (Rancho Dominguez, CA, USA). Amicon® Ultracentrifugal filter devices (MWCO 10k) were from Millipore (Bedford, MA, USA). All other reagents were purchased from Sigma-Aldrich (Ontario, Canada) and used as received, unless otherwise noted.

Characterization

Polymer molecular weights were measured by gel-permeation chromatography (GPC, Viscotek VE2001 GPCmax). Using THF as the mobile phase at a flow rate of 1 ml/min, polymer mass was calculated relative to polystyrene standards. ^{1}H-NMR spectra were recorded on a Varian Mercury 300 spectrometer equipped with SMS sample changer. Dynamic light scattering (DLS) measurements were performed using the Brookhaven 90Plus Particle Sizer (Brookhaven Instruments, Holtsville, NY, USA), which was operated at 674 nm at a scattering angle of 90°. The samples were kept at a constant temperature of 25°C throughout the experiments. Samples contained 4 mg/ml of nanoparticles in distilled water. Cumulant analysis of the scattering data was used to estimate hydrodynamic diameters and polydispersity.

The mean apparent hydrodynamic radius R_h is calculated according to the Stokes–Einstein equation: $R_h = k_B T/6\pi\eta D$, where k_B is the Boltzmann constant, T is the absolute temperature, η is the viscosity of the solvent and D is the mean translational diffusion coefficient. The polydispersity factor is represented as μ_2/Γ^2 where μ_2 is the second cumulant of the decay function and Γ is the average characteristic line width. The polydispersity factor is small (0.020 to 0.080) for narrow distributions and larger for broader distributions. CONTIN algorithms were used to confirm the modality of the particle size distributions. Cryogenic temperature transmission electron microscopy (Cryo-TEM) images were obtained by using a Hitachi S-5200 scanning transmission electron microscopy operating at 200 kV. Samples were prepared by placing one drop of self-aggregated nanoparticle solution (4 mg/ml in distilled water) on a formvar film coated copper grid. After removing excess solution by filter paper, the sample was allowed to air-dry. The temperature was kept below 107 K during the viewing procedure.

Polymer synthesis

*Synthesis of poly(2-methyl, 2-benzyloxycarbonyltrimethylene carbonate)-furan (poly(TMCC-co-LA)-furan) (**3**) (Scheme 1).* Poly(2-methyl-2benzyloxycarbonyl-trimethylene carbonate) (poly(TMCC-*co*-LA)) **1** was synthesized as described before [7]. Co-polymer **1** (6.0 g, 0.4 mmol) was dissolved in 200 ml of ethyl acetate (EtOAc). Dicyclohexylcarbodiimide (DCC, 0.6 g, 2.9 mmol) was added to activate carboxylic acid groups on polymer chains. The reaction solution was stirred for 30 min at room temperature (RT) after which furfurylamine (0.6 g, 6.2 mmol) was added. The reaction mixture was then allowed to stir overnight at RT. The resulting product was precipitated twice in hexane and dried in a vacuum oven overnight at RT. The co-polymer poly(TMCC-*co*-LA)-furan **2** was collected (4.5 g, 0.3 mmol, 75%). ^{1}H-NMR ($CDCl_3$, 300 MHz): δ 1.20–1.35 ppm (bm, C$\underline{H}_3$ protons of the TMC segments), δ 1.40–1.65 ppm (bm, C$\underline{H}_3$ protons of the LA segments), δ 4.20–4.40 ppm (bm, C$\underline{H}_2$ protons of the TMC segments), δ 5.05–5.30 ppm (bm, C$\underline{H}$ protons of the LA segments), δ 7.30–7.40 ppm (bm, CCHCHC$\underline{H}$O protons of the furan groups).

*Synthesis of poly(2-methyl, 2-carboxy trimethylene carbonate-co-*D,L*-lactide-graft-poly(ethylene glycol)-furan (poly(TMCC-co-LA)-g-PEG-furan) (**4**).* Poly(TMCC-*co*-LA)-*g*-PEG-furan was synthesized as described before [7]. Briefly, Co-polymer **1** (100 mg, 6.3 μmol) was dissolved in 5 ml of dimethylformamide (DMF) and 0.5 ml of MES buffer (10 mM, pH 5.5). 10 wt% *N*-ethyl-*N*′-(3dimethylaminopropyl)carbodiimide hydrochloride (EDAC, 52 μmol) and Sulfo-NHS (46 μmol) were added. The reaction solution was incubated at RT for 30 min. 50 mg furan-PEG-NH_2 **2** (15 μmol) was dissolved in 1 ml of a borate buffer solution (500 mM, pH 9.0). This solution was then slowly added to the activated co-polymer **1** solution under stirring. The reaction mixture was incubated at RT for 24 h, after which the reaction solution was dialyzed against distilled water for 24 h

at RT using a dialysis membrane with a MWCO of 12–14 kg/mol. The distilled water was replaced every 2 h for the first 8 h of the dialysis. Self-aggregation of co-polymer **4** during the dialysis process resulted in the formation of nanoparticles. The nanoparticle suspension was purified by passing through a Sepharose 4B column (5 cm diameter × 15 cm length) equilibrated with distilled water. The unreacted PEG was removed as fraction 140–200 ml. The collected nanoparticles (fraction 50–110 ml) were freeze-dried to yield a white solid of co-polymer **4** (75 mg, 3.9 μmol, 50.0%). For furan-PEG-NH_2, ^{1}H-NMR data (DMSO-d_6, 300 MHz): δ 3.45–3.52 ppm (bs, C$\underline{H}_2$ protons of the PEG grafts), δ 6.16–6.21 ppm (bs, 3-C$\underline{H}$ of furan), δ 6.34–6.39 ppm (bs, 4-C$\underline{H}$ of furan), δ 7.51–7.56 ppm (bs, 5-C$\underline{H}$ of furan). For poly(TMCC-*co*-LA)-*g*-PEG-furan, ^{1}H-NMR data (DMSO-d_6, 300 MHz): δ 1.38–1.48 ppm, (bm, C$\underline{H}_3$ protons of the poly(TMCC-*co*-LA) backbone), δ 3.45–3.50 ppm (bs, C$\underline{H}_2$ protons of the PEG grafts), δ 5.05–5.25 ppm (bm, C$\underline{H}_2$ protons of the poly(TMCC-*co*-LA) backbone). Based on the ^{1}H-NMR spectrum of poly(TMCC-*co*-LA)*g*-PEG-furan, it was estimated that there was an average of one PEG graft per co-polymer backbone. The PEG coupling efficiency was 44%, as calculated by comparing the actual PEG grafting density of 1.0 PEG/backbone with the targeting PEG grafting density of 2.3 PEG/backbone. Based on the ^{1}H-NMR spectrum of furan-PEG-NH_2, it was estimated that 84% of PEG molecules contained a furan end group. Therefore, each graft co-polymer molecule contained an average of 0.8 furan groups.

Nanoparticle preparation

Co-polymers were dissolved in DMF to which borate buffer was added (50 mM, pH 9.0, up to 50 vol%) at a polymer concentration of 10 mg/ml. The solution was dialyzed against distilled water using a dialysis membrane with a MWCO of 12–14 kg/mol at RT for 24 h.

Determination of apparent critical aggregation concentration (CAC_{app})

100 μl of pyrene solution (2 ppm in acetone) was added to a 5 ml volumetric vial and the acetone was allowed to evaporate. 2 ml of nanoparticle solution in 10 mM PBS (pH 7.4) at concentrations ranging from 0.1 μg/ml to 40 μg/ml were then added to the vials containing the pyrene residue. All of the polymer solutions contained excess pyrene at a concentration of 0.1 ppm (0.49 μM). The solutions were allowed to incubate at RT for 24 h. Fluorescence spectra of the polymer solutions were then recorded using a Spectra MAX Gemini XS plate reader. The excitation spectra were recorded from 300 nm to 360 nm with an emission wavelength of 390 nm. The excitation bandwidths were set at 1.0 nm.

Encapsulation of DOX and determination of encapsulation efficiency

DOX was incorporated into the nanoparticles by a similar dialysis process as described above.

Briefly, co-polymer and DOX were both dissolved in DMF or a DMF/borate buffer (50 mM, pH 9.0) solvent mixture at a co-polymer concentration of 10 mg/ml and a DOX concentration of 0.1 mg/ml. The solution was dialyzed against distilled water using a dialysis membrane with a MWCO of 12–14 kg/mol at RT for 24 h. After dialysis, the nanoparticle solution was passed through a Sephadex G-25 column equilibrated with PBS buffer (10 mM, pH 7.4) to remove unencapsulated DOX. The content of DOX was determined by dissolving the freeze-dried co-polymer sample in DMSO/H_2O (8:2, v/v) and measuring UV absorbance at 485 nm with a previously established calibration curve. The DOX loading capacity is expressed as the w/w% of the mass of encapsulated DOX within the self-assembled nanoparticles to the mass of nanoparticles.

Stability of DOX-encapsulated nanoparticles in solutions

The stability of DOX-encapsulated nanoparticles was studied by detecting free DOX in the nanoparticle solution in PBS at both 4°C for a period of 2 weeks and 37°C for a period of 48 h. After incubation for various time periods, the nanoparticle solutions were centrifuged using centrifugal filters (membrane MWCO 10 kg/mol) to separate free DOX from the nanoparticles. The free DOX in the centrifuge solution was determined by measuring UV absorbance at 485 nm.

RESULTS AND DISCUSSION

The synthesis of the two types of furan-functionalized co-polymers was carried out as outlined in Scheme 1. As previously reported [7], the poly(TMCC-*co*-LA) backbone was synthesized by ring-opening polymerization of cyclic carbonate monomer, 5-methyl-5-benzyloxycarbonyl-1,3-trimethylene carbonate (benzyl-protected TMCC) and D,L-lactide (LA), yielding the random co-polymer with 13.0 mol% TMCC and 87.0 mol% LA from a molar feed ratio 2:9 of TMCC to LA. The resulting number average molecular weight (M_n), relative to polystyrene standards, was 15.8 kg/mol with a polydispersity estimated at 2.3. Two ways of creating furan-functionalization are described here: (1) direct modification of pendant carboxylic acid groups with furfurylamine to achieve pendant furan groups along the co-polymer chain (co-polymer **3**); and (2) coupling bifunctional furan-PEG-NH_2 to pendant carboxylic acid groups to create furan-terminated PEG graft co-polymers (co-polymer **4**). The furfurylamine modification is a simple and straightforward route to incorporate quantitative furan groups onto the co-polymers, while the PEG-furan grafting creates amphiphilic co-polymers with well-defined hydrophobic and hydrophilic segments for core-shell nanoparticle preparation.

For the poly(TMCC-*co*-LA)-furan co-polymer, the carboxylic acid groups on the polymer backbone were activated by DCC and then coupled with furfurylamine. The furan-functionalized co-polymer was purified by precipitation from ethyl acetate to hexane. The ^{1}H-NMR spectrum (Fig. 1a) confirms the successful furan

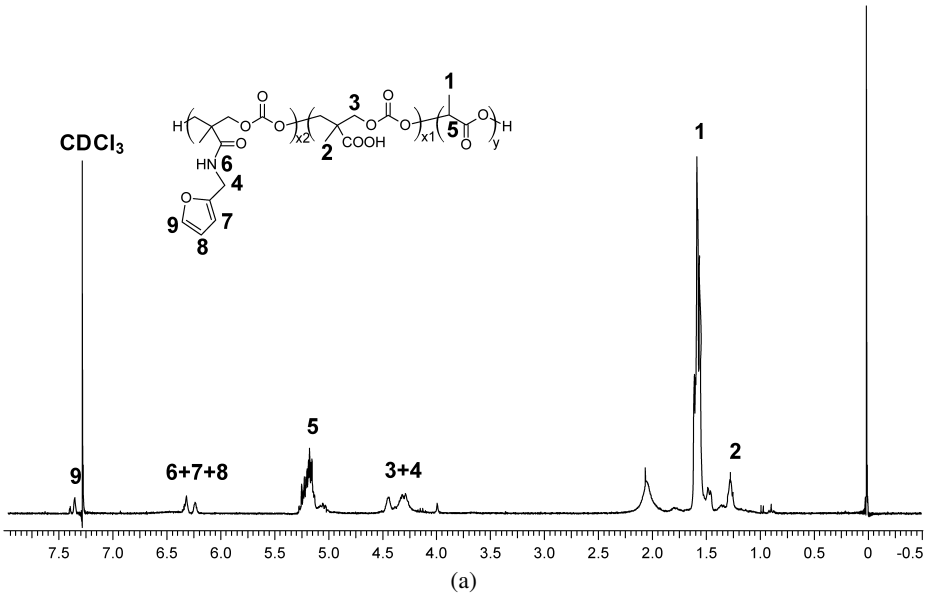

(a)

Figure 1. ^{1}H-NMR spectra of (a) poly(TMCC-*co*-LA)-furan.

modification as the signal at 7.3–7.4 ppm originates from the protons in the furan groups. There were 13.0 mol% of TMCC groups initially present and 5.7 mol% were furan-functionalized, indicating that 44% of total carboxylic acid groups were modified, as determined by ^{1}H-NMR.

For the poly(TMCC-*co*-LA)-*g*-PEG-furan co-polymer, commercially available BocNH-PEG-NHS was first modified with furfurylamine as previously described [7]. The furan-PEG-NH_2 was coupled to the carboxylic acid groups through EDC chemistry. The reaction mixture was dialyzed against distilled water and then passed through a Sepharose 4B gel column to remove unreacted free PEG chains from the self-assembled co-polymer. As shown in Fig. 1b1, the characteristic peaks of furan groups in the ^{1}H-NMR spectrum of furan-PEG-NH_2 indicate the successful furan modification. In the ^{1}H-NMR spectrum of poly(TMCC-*co*-LA)-*g*-PEG-furan (Fig. 1b2), the characteristic peak of PEG appeared at 3.5 ppm, confirming the successful grafting of PEG-furan to the co-polymer backbone. There was an average one PEG-furan graft on each polymer chain as determined by ^{1}H-NMR.

Poly(TMCC-*co*-LA)-furan **3** has a hydrophobic backbone composed of random TMCC and LA units. The hydrophilic pendant carboxylic acid groups, however, provide amphilicity to the co-polymer. Poly(TMCC-*co*-LA)-*g*-PEG-furan exhibits well-defined hydrophobic/hydrophilic segments: a hydrophobic poly(TMCC-*co*-LA) backbone and hydrophilic PEG grafts. Since both of the co-polymers may have the capacity to self-assemble in aqueous environments, dialysis was pursued as it is one of the principal methods for the preparation of self-assembled polymeric nanoparticles [1, 2, 16, 20]. By dissolving amphiphilic co-polymers in a common organic solvent that is miscible with water and dialyzing against aqueous solution,

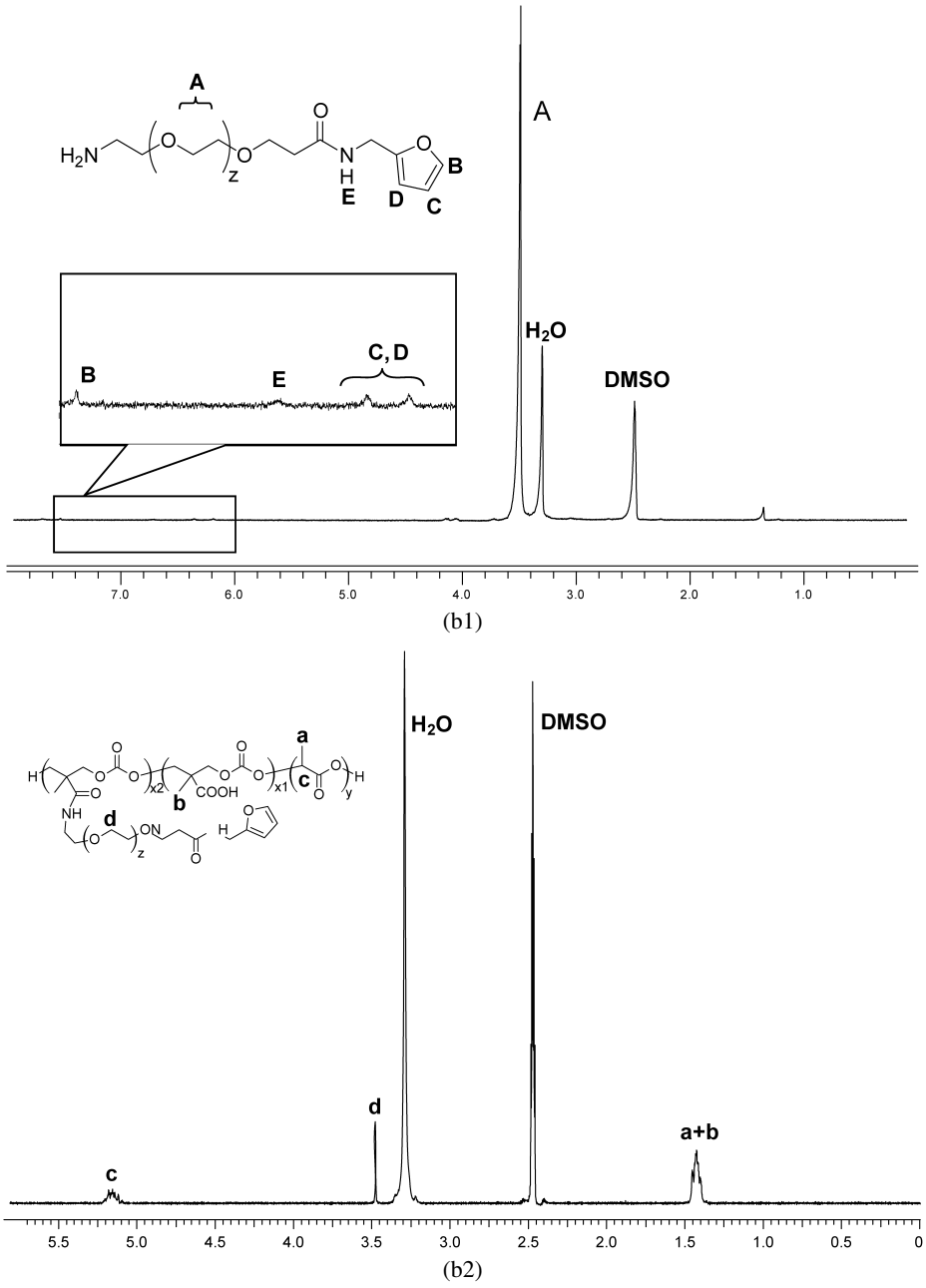

Figure 1. (Continued.) (b1) Furan-PEG-NH_2 and (b2) poly(TMCC-*co*-LA)-*g*-PEG-furan.

the formation of self-assembled structures is induced during solvent exchange. To verify this hypothesis, the two polymers were dissolved in dimethylformamide (DMF) at a concentration of 10 mg/ml and dialyzed against distilled water. It was found that both poly(TMCC-*co*-LA)-furan and poly(TMCC-*co*-LA)-*g*-PEG-furan

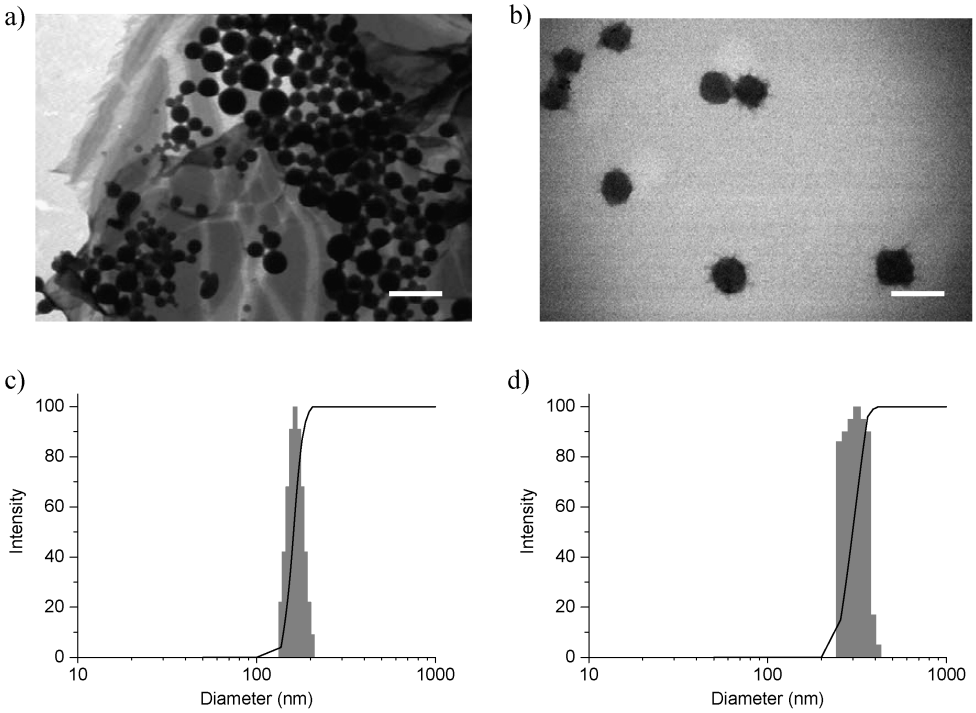

Figure 2. Cyro-TEM images of (a) poly(TMCC-*co*-LA)-furan and (b) poly(TMCC-*co*-LA)-*g*-PEG-furan self-assembled nanoparticles (size bar = 500 nm), and CONTIN analysis of particle diameter and size distribution of (c) poly(TMCC-*co*-LA)-furan and (d) poly(TMCC-*co*-LA)-*g*-PEG-furan self-assembled nanoparticles as obtained by DLS.

self-assembled into nanoparticles with a spherical aggregation morphology (Fig. 2a and 2b). Using DLS, the mean effective hydrodynamic diameter and polydispersity was calculated by the cumulant method and the modality of the size distribution was determined by CONTIN analysis. The hydrodynamic diameters of poly(TMCC-*co*-LA)-furan and poly(TMCC-*co*-LA)-*g*-PEG-furan nanoparticles were 169 nm and 283 nm, respectively. The poly(TMCC-*co*-LA)-*g*-PEG-furan nanoparticles had larger overall diameters than the poly(TMCC-*co*-LA)-furan nanoparticles because the grafted PEG chains were likely oriented toward the aqueous solution and associated with interior swelling. The polydispersity was fairly high for both types of nanoparticles (0.17 for poly(TMCC-*co*-LA)-furan nanoparticles and 0.21 for poly(TMCC-*co*-LA)-*g*-PEG-furan nanoparticles), indicating a relatively broad size distribution. The CONTIN analysis in Fig. 2c and 2d suggests that the particle distribution was unimodal.

The formation of hydrophobic microdomains in the self-assembled nanoparticles was confirmed by incubating dilute nanoparticle solutions with a hydrophobic fluorescent probe, pyrene [3, 4, 10, 11]. When exposed to the nanoparticle solution, the hydrophobic pyrene molecules preferably partition inside the hydrophobic microdomains resulting in different photophysical characteristics compared to those

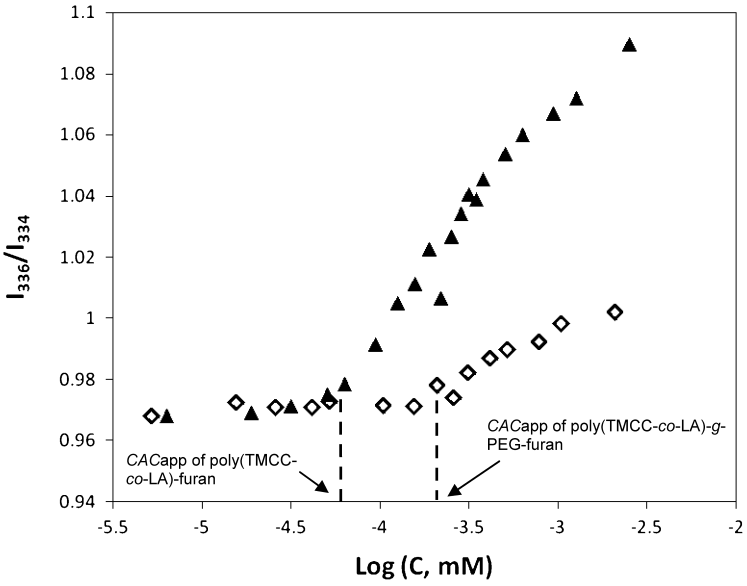

Figure 3. Intensity ratio (I_{336}/I_{334}) obtained from the fluorescence excitation spectra of pyrene plotted *versus* (▲) co-polymer poly(TMCC-*co*-LA)-furan and (◊) poly(TMCC-*co*-LA)-*g*-PEG-furan concentration. The CAC_{app} is shown as the onset of the changes of the I_{336}/I_{334}.

of free pyrene molecules. The red-shift of the pyrene (0,0) band from 334 nm to 336 nm reflects the partitioning of pyrene into the hydrophobic region of the micellar nanoparticles (data not shown). Figure 3 shows the I_{336}/I_{334} intensity ratio of the pyrene excitation spectra *versus* the logarithm of the co-polymer concentration. The cross-over points at the low concentration ranges indicate the apparent critical aggregation concentration (CAC_{app}) which is the minimum co-polymer concentration required for the formation of self-assembled structures. It was determined that the CAC_{app} of poly(TMCC-*co*-LA)-furan (approximately 50 nM) was much lower than that of poly(TMCC-*co*-LA)-*g*-PEGfuran (200 nM), suggesting stronger associations among the polymer chains of poly(TMCC-*co*-LA)-furan due to the lack of hydrophilic PEG chains. Both of the CAC_{app} values are significantly lower than those of low-molecular-weight surfactants and comparable to those of reported amphiphilic co-polymers [1, 3, 4, 10]. Considering that the CAC value is an indication of thermodynamic stability of self-assembled systems under extremely dilute conditions, it is expected that limited dissociation may occur when these nanoparticles are used as drug-delivery vehicles for *in vivo* applications.

The size of polymeric nanoparticles is critical for their application as efficient drug carriers and crossing the leaky vasculature that surrounds cancerous tissue. Particle size impacts drug encapsulation, stability and storage [1]. Larger sizes may facilitate higher drug loading while smaller sizes have the advantage of easy sterilization by simple filtration [21, 22]. For intravenous circulation, extravasation and intracellular localization are sensitive to nanoparticle size [25–28]. The sizes

of polymeric self-assembled nanoparticles depend on several factors including co-polymer molecular weight, relative proportion of hydrophilic and hydrophobic chains and processing procedures [1, 6, 21, 22]. However, achieving a broad size range of self-assembled nanoparticles from the same polymer and controlling the size by dialysis have not been reported.

In this study, both poly(TMCC-*co*-LA)-furan and poly(TMCC-*co*-LA)-*g*-PEG-furan were self-assembled into nanoparticles in aqueous environments driven by the hydrophobic association among polymer chains. These associations were controlled by the addition of an alkaline buffer component to the organic solvent used to dissolve the co-polymers during the dialysis procedure, thereby resulting in different particle sizes. For example, dialyzing poly(TMCC-*co*-LA)-furan co-polymer solution in pure DMF resulted in self-assembled nanoparticles of 169 nm in diameter (Fig. 4a). After the addition of 5 vol% of borate buffer (50 mM, pH 9.0) to the DMF, the hydrodynamic diameter of the self-assembled nanoparticles was reduced to 146 nm. Increasing the volume ratio of borate buffer resulted in decreased particle size. When the borate buffer in the solvent mixture reached at 50 vol%, the dialysis procedure resulted in self-assembled nanoparticles as small as 54 nm (Fig. 4a). The same trend was observed with poly(TMCC-*co*-LA)-*g*-PEG-furan co-polymer (Fig. 4b). As the borate buffer volume ratio increased from 0 vol% to 50 vol% in the solvent mixture, the hydrodynamic diameters of poly(TMCC-*co*-LA)-*g*-PEG-furan nanoparticles decreased from 283 nm to 28 nm. The same trends in nanoparticle diameter were observed by Cyro-TEM where the spherical shape and dense inner structure for these nanoparticles were also observed (images not shown). As described previously, the nanoparticles dimensions by TEM and DLS are consistent [7].

We attribute this feature of nanoparticle size control with the addition of borate buffer to the presence of carboxylic acid substituents in the co-polymers because the carboxylic acid groups were ionized in an alkaline environment of pH 9.0. The degree of ionization of the carboxylic acid groups increased with the increasing volume ratio of borate buffer in the solvent mixture, resulting in increased electrostatic repulsion among the co-polymer chains. At the same time, the hydrophilicity of the co-polymer backbone was enhanced by the ionization of the carboxylic acid groups. Therefore, the overall hydrophobic association among polymer chains became weaker with the increased addition of borate buffer. Stronger repulsive interactions and weaker hydrophobic associations resulted in fewer polymer chains aggregating to form a nanoparticle, which correlated with smaller hydrodynamic diameters. While alkaline pH is known to enhance poly(lactide) degradation, it is unlikely that the <25 mM borate buffer solutions used to create the nanoparticles and the short exposure time (<6 h) resulted in polymer degradation [23, 24].

For intravenous delivery, nanoparticles with diameters less than 200 nm are believed to be less susceptible to reticuloendothelial system (RES) clearance and, thus, to have a prolonged circulation time and greater opportunity for accumulation in cancerous tissues [1, 25–27, 29]. Interestingly, very small particles (for example,

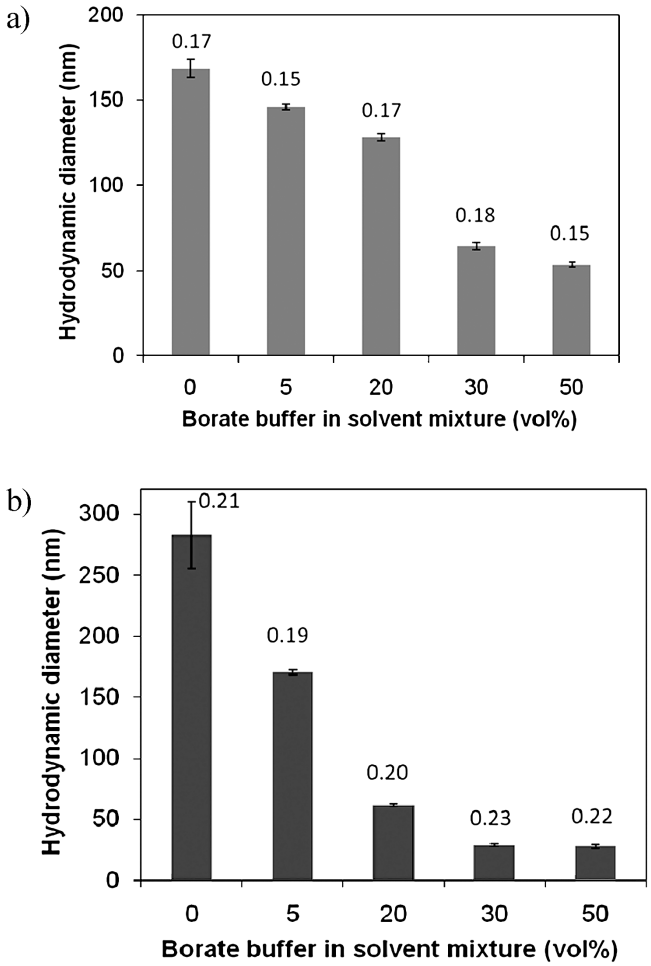

Figure 4. Changes of hydrodynamic diameter of self-assembled nanoparticles of (a) poly(TMCC-*co*-LA)-furan and (b) poly(TMCC-*co*-LA)-*g*-PEG-furan as a function of volume percentage of borate buffer in the solvent mixture. Shown are the mean hydrodynamic diameters of three measurements ± SD by DLS. The numbers provided are the polydispersities of particle size.

PEG-liposomes < 70 nm) did not exhibit favorable accumulation in cancerous tissue compared to larger ones of 100–200 nm [25, 28]. Our ability to control nanoparticle size will allow us to test its importance for both formulations: (1) poly(TMCC-*co*-LA)-furan nanoparticles with diameters of 54–169 nm and (2) poly(TMCC-*co*-LA)-*g*-PEG-furan nanoparticles with diameters of 28–283 nm. These formulations will also allow us to test the importance of the PEG grafts to circulation time where PEG has been shown to limit macrophage engulfment.

The encapsulation of hydrophobic drugs within the self-assembled polymeric nanoparticles through drug–polymer hydrophobic interaction has been well-established [2, 3, 12, 14, 18, 20]. The drug-loading capacity is influenced by the properties

of the drugs and the co-polymers. To verify the capability of our polymer system to encapsulate drugs, we investigated the effect of nanoparticle size on drug-loading capacity using the hydrophobic anticancer drug doxorubicin (DOX, 0.544 kg/mol). DOX is a DNA-interacting drug widely used in chemotherapy; however, low water solubility, rapid clearance during circulation and systemic toxicity limit its therapeutic efficacy. Incorporation of DOX within the polymeric nanoparticles is expected to overcome these shortcomings and achieve intracellular delivery by antibody-mediated endocytosis.

DOX was encapsulated in the nanoparticles during the self-assembly dialysis procedure. The DOX-encapsulated nanoparticles had similar size as the blank nanoparticles. Increasing borate buffer in the solvent mixture induced larger DOX-encapsulated nanoparticles. To determine the amount of DOX incorporated into the self-assembled nanoparticles, the DOX-loading capacity was defined as:

$$\text{DOX-loading capacity (\%, w/w)} = \left(\frac{\text{mass of DOX in nanoparticles (mg)}}{\text{mass of nanoparticles (mg)}} \right) \times 100\%.$$

Figure 5 shows the DOX-loading capacities plotted *versus* the volume ratio of borate buffer in the solvent mixture during dialysis. Adjusting the volume ratio of borate buffer in solvent mixture during the dialysis procedure not only varied particle size but also affected drug loading. DOX-loading capacity decreased as the volume ratio of borate buffer increased for both of the co-polymers, indicating that larger nanoparticles encapsulated higher amounts of DOX. The trends are

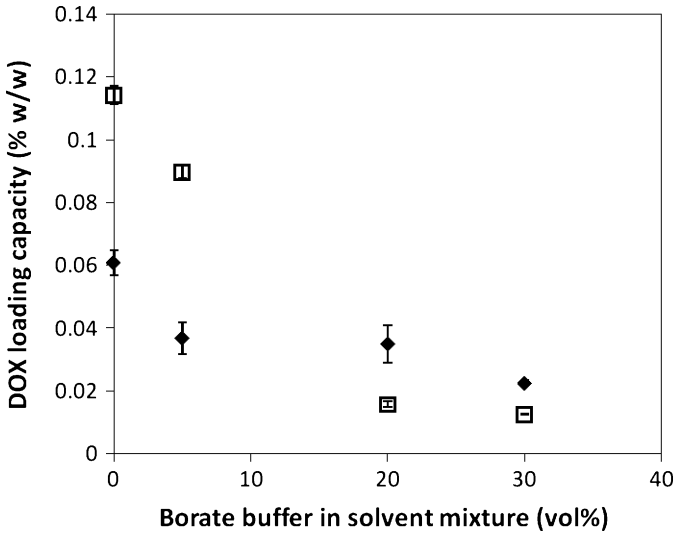

Figure 5. DOX-loading capacity in self-assembled nanoparticles from poly(TMCC-*co*-LA)-furan (♦) and poly(TMCC-*co*-LA)-*g*-PEG-furan (□) as a function of volume percentage of borate buffer in the solvent mixture. Shown are the mean value of three measurements ± SD.

consistent with those reported by other groups that larger nanoparticles incorporate greater amounts of hydrophobic drugs [21, 22]. This effect is likely attributed to the larger inner hydrophobic domain in larger diameter nanoparticles. The drug-loading capacity in our nanoparticle systems (up to 0.06% (w/w) for poly(TMCC-*co*-LA)-furan and 0.1% (w/w) for poly(TMCC-*co*-LA)-*g*-PEG-furan) is lower than those of self-assembled block co-polymeric nanoparticles with similar sizes [12, 21]. The randomly distributed carboxylic acid groups present on our polymer backbone likely diminish the formation of a complete hydrophobic core and effective association between DOX and the hydrophobic domains. However, the presence of carboxylic acid groups within the polymeric nanoparticles is likely a considerable advantage for the encapsulation of protein drugs or cationic drugs which may form drug-polymer complexes through hydrogen bonding and electrostatic interactions [30, 31].

The stability study has revealed that there was little DOX released from all of the nanoparticle samples at 4°C over a period of 2 weeks, indicating nanoparticle stability when stored under these conditions. Importantly, there was no significant DOX released at 37°C over a period of 48 h, suggesting that this nanoparticle delivery system can be used in a targeted delivery strategy. Since DOX is a highly potent and highly toxic chemotherapeutic, it is preferable to deliver DOX intracellularly to targeted cancerous cells. Using antibody-mediated endocytosis, these encapsulated DOX nanoparticles may be used in a targeted delivery strategy where reduced systemic toxicity (due to the lack of DOX diffusion at 37°C) and enhanced drug efficiency at the target sites may be achieved.

CONCLUSIONS

We have successfully developed two types of furan-functionalized co-polymers poly(TMCC-*co*-LA)-furan and poly(TMCC-*co*-LA)-*g*-PEG-furan. The co-polymers are able to self-assemble into nanoparticle structures driven by dialysis. By adjusting the amount of borate buffer added in the organic solvent during the dialysis procedure, the hydrodynamic diameters of the self-assembled nanoparticles were controlled over a broad size range. Encapsulation of DOX within these nanoparticles demonstrates the capability of the nanoparticles to deliver hydrophobic anti-cancer drugs. Given the importance of nanoparticle size and the ability to covalently bind targeting ligands, this nanoparticle system holds great promise as a highly efficient delivery vehicle for targeted anti-cancer drug delivery.

REFERENCES

1. C. Allen, D. Maysinger and A. Eisenberg, *Colloids Surface B* **16**, 3 (1999).
2. E. K. Park, S. Y. Kim, S. B. Lee and Y. M. Lee, *J. Control. Rel.* **109**, 158 (2005).
3. F. Wang, T. K. Bronich, A. V. Kabanov, R. D. Rauh and J. Roovers, *Bioconjug. Chem.* **16**, 397 (2005).

4. F. Zang, H. Lee and C. Allen, *Bioconjug. Chem*. **17**, 399 (2006).
5. H. Arimura, Y. Ohya and T. Ouchi, *Biomacromolecules* **6**, 720 (2005).
6. J. Cheng, B. A. Teplya, I. Sherifia, J. Sunga, G. Luthera, F. X. Gua, E. Levy-Nissenbauma, A. F. Radovic-Morenob, R. Langer and O. C. Farokhzad, *Biomaterials* **28**, 869 (2007).
7. M. Shi, J. H. Wosnick, K. Ho, A. Keating and M. S. Shoichet, *Angew. Chem. Int. Edn* **46**, 6126 (2007).
8. N. Nasongkla, E. Bey, J. Ren, H. Ai, C. Khemtong, J. S. Guthi, S. F. Chin, A. D. Sherry, D. A. Boothman and J. Gao, *Nano Lett.* **6**, 2427 (2006).
9. R. Kuma, M. H. Chen, V. S. Parmar, L. A. Samuelson, J. Kumar, R. Nicolosi, S. Yoganathan and A. C. Watterson, *J. Am. Chem. Soc.* **126**, 10640 (2004).
10. S. Kwon, J. H. Park, H. Chung, I. C. Kwon and S. Y. Jeong, *Langmuir* **19**, 10188 (2003).
11. M. Wilhelm, C. L. Zhao, Y. Wang, R. Xu, M. A. Winnik, J. L. Mura, G. Riess and M. D. Croucher, *Macromolecules* **24**, 1033 (1991).
12. P. L. Soo, L. Luo, D. Maysinger and A. Eisenberg, *Langmuir* **18**, 9996 (2002).
13. P. N. Zawaneh, A. M. Doody, A. N. Zelikin and D. Putnam, *Biomacromolecules* **7**, 3245 (2006).
14. E. R. Gillies and J. M. J. Fréchet, *Bioconjug. Chem.* **16**, 361 (2005).
15. E. S. Lee, K. Na and Y. H. Bae, *Nano Lett.* **5**, 325 (2005).
16. G. M. Kim, Y. H. Bae and W. H. Jo, *Macromol. Biosci.* **5**, 1118 (2005).
17. K. Akiyoshi, E. C. Kang, S. Kurumada, J. Sunamoto, T. Principi and F. M. Winnik, *Macromolecules* **33**, 3244 (2000).
18. V. P. Torchilin, A. N. Lukyanov, Z. Gao and B. Papahadjopoulos-Sternberg, *Proc. Natl. Acad. Sci. USA* **100**, 6039 (2003).
19. T. M. Allen, *Nature Rev. Cancer* **2**, 750 (2002).
20. Y. Bae, N. Nishiyama, S. Fukushima, H. Koyama, M. Yasuhiro and K. Kataoka, *Bioconjug. Chem.* **16**, 122 (2005).
21. W. Wang, L. Tetley and I. F. Uchegbu, *Langmuir* **16**, 7859 (2000).
22. Y. Yoo, D. C. Kim and T. Y. Kim, *J. Appl. Polym. Sci.* **74**, 2856 (1999).
23. T. Shirahasea, Y. Komatsua, Y. Tominagaa, S. Asaia and M. Sumita, *Polymer* **47**, 4839 (2006).
24. C. S. Chaw, K. W. Chooi, X. M. Liu, C. Tan, L. Wang and Y. Y. Yang, *Biomaterials* **25**, 4297 (2004).
25. O. Ishida, K. Maruyama, K. Sasaki and M. Iwatsuru, *Int. J. Pharm.* **190**, 49 (1999).
26. B. Pegaz, E. Debefve, J. P. Ballini, Y. N. Konan-Kouakou and H. van den Bergh, *J. Photochem. Photobiol. B* **85**, 216 (2006).
27. M. El-Sayed, M. F. Kiani, M. D. Naimark, A. H. Hikal and H. Ghandehari, *Pharm. Res.* **18**, 23 (2001).
28. D. C. Litzinger, A. M. J. Buiting, N. van Rooijen and L. Huang, *Biochim. Biophys. Acta* **1190**, 99 (1994).
29. S. M. Moghimi, A. C. Hunter, and J. C. Murray, *Pharmacol. Rev.* **53**, 283 (2001).
30. T. Ehtezazi, T. Govender and S. Stolnik, *Pharm. Res.* **17**, 871 (2000).
31. T. Govender, T. Ehtezazi, S. Stolnik, L. Illum and S. S. Davis, *Pharm. Res.* **16**, 1125 (1999).